# A new coupled-map car-following model based on a transportation supernetwork framework*

Yao Jing(姚 静)[a)b)†], Huang Jing-Yi(黄婧祎)[a)], Chen Guan-Rong(陈关荣)[c)], and Xu Wei-Sheng(许维胜)[a)]

[a)] *Department of Control Science and Engineering, Tongji University, Shanghai* 201804, *China*
[b)] *Department of Electronic and Computer Engineering, The Hong Kong University of Science and Technology, Hong Kong SAR, China*
[c)] *Department of Electronic Engineering, City University of Hong Kong, Hong Kong SAR, China*

(Received 24 November 2012; revised manuscript received 21 January 2013)

A new car-following model is proposed by considering information from a number of preceding vehicles with inter-vehicle communication. A supernetwork architecture is first described, which has two layers: a traffic network and a communication network. The two networks interact with and depend on each other. The error dynamic system around the steady state of the model is theoretically analyzed and some nonjam criteria are derived. A simple control signal is added to the model to analyze the criteria of suppressing traffic jams. The corresponding numerical simulations confirm the correctness of the theoretical analysis. Compared with previous studies concerning coupled map models, the controlled model proposed in this paper is more reasonable and also more effective in the sense that it takes into account the formation of traffic congestion.

**Keywords:** traffic flow, coupled map car-following model, inter-vehicle communication, supernetwork

**PACS:** 02.60.Cb, 05.20.Dd, 05.45.Ra, 89.04.–a **DOI:** 10.1088/1674-1056/22/6/060208

## 1. Introduction

In the past half a century, traffic flow problems have been widely investigated in the field of physics.[1–5,7–14] Many models have been proposed and developed to study the mechanism of traffic congestion and its control methods. The car-following model is one of the microscopic traffic flow models, first proposed by Reushel and Pipes in the 1950s.[1,2] This classical car-following model describes the motion of a vehicle following the front vehicle in a single lane of traffic, which can well describe the movement of individual vehicles in a traffic flow system.

In 1961, Newell[3] introduced the concept of optimal velocity (OV). In 1995, Bando *et al.*[4] proposed an optimal velocity (OV) model, described by a simple differential equation including an OV function. In the model, every vehicle has an optimal velocity produced by the OV function, depending on the headway distance of the current vehicle. It shows the traffic jam phenomenon under periodic boundary conditions and derives a simple stability condition. In 1998, Helbing and Tilch[5] identified some parameters of the OV model according to the data from real traffic systems and developed a generalized force (GF) model, which solves the problem of some unreasonable values of acceleration produced by the OV model. In 2002, to improve the GF model, Jiang *et al.*[6] proposed a new continuum model, which overcomes a problem that the characteristic speeds are greater than the macroscopic flow.

In recent years, the coupled map (CM) car-following model has played an important role in suppressing traffic jams. It not only represents the traffic phenomena in a simple way, but also takes a short time in computer simulation. In 1999, Konishi *et al.*[7] proposed a CM model and suggested a delayed-feedback control method to suppress the traffic jams. They investigated the noise effects under open boundary bottleneck conditions on computer simulations, showing that the traffic system could run well under control. In 2006, Zhao[8] presented a similar but more effective and simpler method for suppressing traffic congestion. In 2007, Han *et al.*[9] proposed a control scheme with application to intelligent transportation systems (ITS). They designed the control signal to include the velocity information of a number of preceding vehicles. In 2009, Han *et al.*[10] proposed a modified CM model based on previous works, considering both forward- and backward-looking information. In 2011, Ge *et al.*[11] modified the OV function of the CM model proposed in Ref. [7]. The optimal velocity produced by the new function depends not only on the headway distance of the current vehicle but also on the preceding one's. Some research related to the CM car-following model and the associated control methods have been extensively studied lately.[12–14]

Recently, several car-following models based on ITS have

*Project supported by the National Natural Science Foundation of China (Grant Nos. 61174158, 61034004, 91024023, and 61272271), the Special Fund from the China Postdoctoral Science Foundation (Grant No. 201104286), the China Postdoctoral Science Foundation (Grant No. 2012M510117), the Natural Science Foundation Program of Shanghai (Grant No. 12ZR1434000), the Fundamental Research Funds for the Central Universities, and the Hong Kong Research Grants Council (Grant No. GRF Grant CityU1109/12).

†Corresponding author. E-mail: yaojing@tongji.edu.cn

© 2013 Chinese Physical Society and IOP Publishing Ltd 

been proposed by taking into account the information of multiple preceding leading vehicles in the traffic flows. [9,10,16–20] All of them assumed that a vehicle could receive information from an arbitrary number of preceding or following vehicles. That is, the connectivity, which is defined to be the probability of being connected, between any two vehicles within a certain range is always supposed to be 1. However, this assumption is not reasonable in practical situations. In ITS, vehicles equipped with wireless devices form a mobile ad hoc network, and the information could be relayed by the equipped vehicles from the information senders to the receivers, which is referred to as inter-vehicle communication (IVC).[20]

In this paper, a new coupled map car-following model considering multiple preceding vehicles under IVC is proposed. Since vehicles usually move at high speeds, some existing links may fail to stay connected due to entering and leaving vehicles in roadway segments. Here, the connectivity is considered under IVC to be in the range of 0 to 1, which depends on the proportion of IVC-equipped vehicles (with a market penetration rate $\mu$) and the transmission range $R$ of the communication devices. For one vehicle, the connectivity determines the amount of the preceding vehicles' information that has effects on the adjustment of the vehicle's velocity. On the other hand, the connectivity under IVC is influenced by preceding vehicles' movement. Thus, a framework of transportation supernetwork[21] is first proposed, in which there are two interdependent networks: transportation network and communication network. The coupled relationship between the two networks is formulated in the proposed CM model. In theoretical analysis, the nonjam criteria are derived, and a simple control signal is designed.

This paper is organized as follows. In Section 2, a new coupled map car-following model is proposed and its stability conditions are derived. In Section 3, a simple control method and its theoretical analysis of stability are given. In Section 4, numerical simulations are performed to verify the theoretical results. Section 5 summarizes the paper.

## 2. Modeling and stability analysis

### 2.1. CM car-following model under IVC

In the car-following model, the leading vehicle is described by

$$x_0(n+1) = v_0 T + x_0(n), \tag{1}$$

where $x_0(n) > 0$ is the position of the leading vehicle at time $t = nT$, $v_0 > 0$ is its velocity which is a constant, and $T > 0$ is the sampling time. Assume that the leading vehicle is not influenced by other vehicles. The following vehicles are described by

$$x_i(n+1) = v_i(n)T + x_i(n), \quad i = 1,2,\ldots,N, \tag{2}$$

where $x_i(n) > 0$ is the position of the $i$-th vehicle at time $t = nT$, $v_i(n) > 0$ is its speed at time $t = nT$, and $N$ is the number of the following vehicles.

Define the $i$-th vehicle's headway distance as $y_i(n) = x_{i-1}(n) - x_i(n)$. In view of inter-vehicle communications, a new coupled map car-following model is formulated as

$$\begin{aligned} v_i(n+1) &= \alpha_i \left\{ \sum_{j=1}^{i} w_{ij} D_{ij} \left[ V_j^{\mathrm{op}}(y_j(n)) - v_i(n) \right] \right\} T \\ &\quad + v_i(n), \end{aligned} \tag{3}$$

$$y_i(n+1) = v_{i-1}(n)T - v_i(n)T + y_i(n), \tag{4}$$

where $\alpha_i > 0$ is the sensitivity of the $i$-th vehicle's driver, $w_{ij}$ is the weight of the $i$-th vehicle's car-following effect due to the $j$-th vehicle ($i \geq j$), and the other parameters will be defined below.

Obviously, in real traffic systems, $w_{ij}$ should satisfy two conditions: (i) $w_{ij}$ reduces gradually as the distance between vehicles $j$ and $i$ increases; (ii) $\sum_{j=1}^{i} w_{ij} = 1$. Considering that the effect from nearby vehicles is much larger than those from far away, the hyperbolic tangent function is used to describe the weight function, instead of the linear function. Specifically the weight $w_{ij}$ is defined as

$$\begin{aligned} w'_{ij} &= \Omega_i(j) = \frac{1}{2}\left[ \tanh 5\left( \frac{j}{i} - \frac{1}{2} \right) + 1 \right], \\ w_{ij} &= \frac{w'_{ij}}{\sum_{j=1}^{i} w'_{ij}}, \qquad j = 1,2,\ldots,i, \end{aligned} \tag{5}$$

where $\Omega_i(j)$ is an increasing function of $j$, ranging from 0 to 1, and $w_{ij}$ is the normalized value of $w'_{ij}$, as illustrated by Fig. 1.

In Eq. (3), $D = (D_{ij})_{N\times N}$ is the coupling configuration matrix, representing the connection from the $j$-th vehicle to the $i$-th one under IVC. If the $i$-th vehicle can receive information from the $j$-th one through multi-hop communications, then $D_{ij} = 1$ $(i > j)$; otherwise, $D_{ij} = 0$. When $i = j$, $D_{ij} = D_{ji} = 1$. And the probability of $D_{ij} = 1$ equals the multi-hop connectivity $S_{ij}$ under IVC, i.e., $P\{D_{ij} = 1\} = S_{ij}$. Here, the connectivity $S_{ij}$ is defined as the probability for the connection from the $j$-th vehicle to the $i$-th one, which depends on the proportion of IVC-equipped vehicles (market penetration rate $\mu$) and the transmission range $R$ of the communication devices as well as the vehicles' movements.[20] Since the model is developed under a single traffic lane without overtaking, the distribution of vehicles would not change significantly. Here, assume that $D$ is a constant matrix, determined by the initial distribution of vehicles' positions.

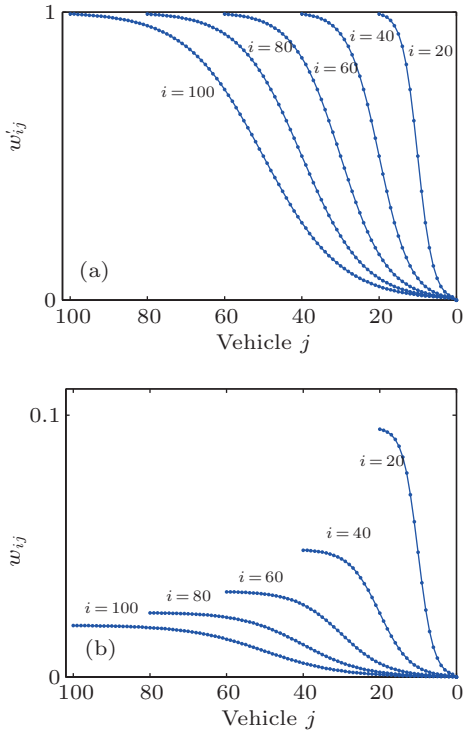



**Fig. 1.** (color online) Illustration of weight functions in the CM model (3). (a) The weight function $w'_{ij}$ for $i = 20, 40, 60, 80, 100$. (b) The weight function $w_{ij}$ for $i = 20, 40, 60, 80, 100$.

And, in Eq. (3), $V_i^{\mathrm{op}}(y_i(n))$ is the optimal velocity (OV) function, defined by

$$V_i^{\mathrm{op}}(y_i(n)) = \frac{v_i^{\max}}{2}\left[1 + \bar{H}_{\mathrm{sat}}\left(2\frac{y_i(n) - \eta_i}{\zeta_i}\right)\right], \tag{6}$$

where $v_i^{\max} > 0$ is the $i$-th vehicle's maximum speed, $\eta_i > 0$ is the neutral headway distance, and $\zeta_i > 0$ is a parameter of the headway distance. The saturation function $\bar{H}_{\mathrm{sat}}(\cdot)$ is defined by

$$\bar{H}_{\mathrm{sat}}(\rho) = \begin{cases} +1, & \rho > +1, \\ \rho, & -1 \le \rho \le +1, \\ -1, & \rho < -1. \end{cases} \tag{7}$$

Assume that the leading vehicle's speed $v_0$ is less than the maximum speed of all the following vehicles, i.e., $v_0 < v_i^{\max}$ $(i = 1, 2, \ldots, N)$, in order to guarantee the existence of all vehicles as a group. To avoid possible collisions and backward motions, we further assume that the $i$-th vehicle can stop suddenly when the headway distance $y_i(n)$ is less than the minimum safety distance $y_i^{\min} > 0$.

### 2.2. Framework of the transportation supernetwork

This new CM car-following model under IVC is a simple supernetwork model, which can be graphically represented as a network of networks (Fig. 2). Here, a two-layer interacting network is presented: the transportation network and the communication network. Vehicles are nodes in the transportation network, within which the correlation of any two nodes is represented by a weighted coupling strength $w_{ij}$. Whereas in the communication network, nodes are IVC-equipped vehicles, and each pair of two nodes is randomly connected by the connectivity $S_{ij}$. The connected state between two nodes is represented by $D_{ij} = 1$, which determines the topological structure of the communication network. The two networks influence each other. The coupling configuration matrix $D$ of the communication network depends on the location distribution of nodes in a traffic network,[16] and the movement of the nodes (hence, their locations) depends on $D$, as formulated by Eq. (3).

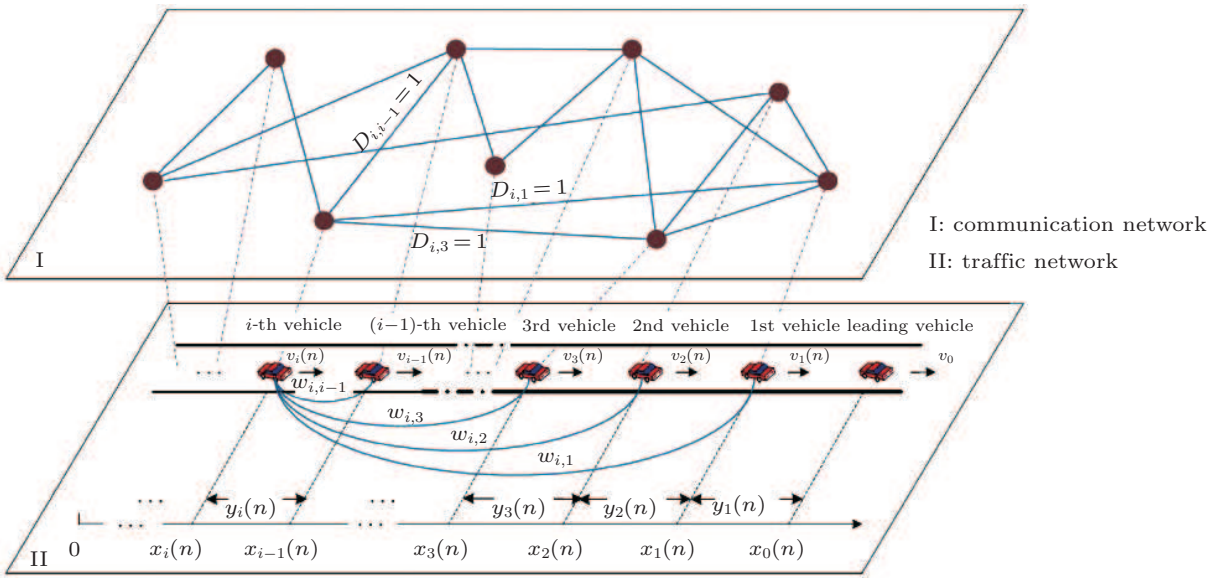



**Fig. 2.** (color online) Framework of the transportation supernetwork.

### 2.3. Stability analysis

Assume that the leading vehicle runs with a constant speed $v_0$, and the following vehicles have the following steady states:[7]

$$[v_i^*,\ y_i^*]^{\mathrm{T}} = \left[v_0,\ \frac{v_0}{r_i} - \frac{\zeta_i}{2} + \eta_i\right]^{\mathrm{T}}, \tag{8}$$

where $r_i = v_i^{\max}/\zeta_i$. Obviously, a necessary and sufficient condition for the existence of the steady state is $v_0 < v_i^{\max}$, $i = 1,2,\ldots,N$.

To normalize the variables and unify their dimensions, define $\mathrm{d}v_i(n) = \delta v_i(n)/v_0$ and $\mathrm{d}y_i(n) = \delta y_i(n)/y_0$, where $v_0 = v_i^*$, $y_0 = \min\{y_i^*\}$, $\delta v_i(n) = v_i(n) - v_0$, and $\delta y_i(n) = y_i(n) - y_0$, $i = 1,2,\ldots,N$.

Then, a perturbation model around the steady state (8) is given by

$$\mathrm{d}v_i(n+1) = \frac{Ty_0}{v_0}\alpha_i \sum_{j=1}^{i} w_{ij}D_{ij}r_j\,\mathrm{d}y_j(n) + \left(1 - T\alpha_i \sum_{j=1}^{i} w_{ij}D_{ij}\right)\mathrm{d}v_i(n), \tag{9}$$

$$\mathrm{d}y_i(n+1) = \frac{Tv_0}{y_0}\,\mathrm{d}v_{i-1}(n) - \frac{Tv_0}{y_0}\,\mathrm{d}v_i(n) + \mathrm{d}y_i(n), \tag{10}$$

which can be rewritten as the following linear state-space model

$$x_i(n+1) = A_i x_i(n) + B_i q_i(n), \tag{11}$$

$$\mathrm{d}v_i(n) = Cx_i(n), \tag{12}$$

where

$$x_i(n) = [\mathrm{d}v_i(n)\ \ \mathrm{d}y_i(n)]^{\mathrm{T}} \in R^2,$$

$$q_i = [\mathrm{d}v_{i-1}(n)\ \ \mathrm{d}y_{i-1}(n)\ \ \ldots\ \ \mathrm{d}y_1(n)]^{\mathrm{T}} \in R^N,$$

$$A_i = \begin{bmatrix} 1 - T\alpha_i \sum\limits_{j=1}^{i} w_{ij}D_{ij} & \dfrac{Ty_0}{v_0}\alpha_i w_{ii} r_i \\ -\dfrac{Tv_0}{y_0} & 1 \end{bmatrix} \in R^{2\times 2},$$

$$B_i = \begin{bmatrix} 0 & \frac{Ty_0}{v_0}\alpha_i w_{i,i-1}D_{i,i-1}r_{i-1} & \ldots & \dfrac{Ty_0}{v_0}\alpha_i w_{i,1}D_{i,1}r_1 \\ \dfrac{Tv_0}{y_0} & 0 & \ldots & 0 \end{bmatrix} \in R^{2\times N},$$

$$C = [1\ \ 0].$$

According to control theory, the conditions of no traffic jams, derived by Konishi *et al.*,[7] are as follows: i) $P_i(z)$ is stable; ii) $\max\limits_{|z|=1} |\, G_i(z)\,| \le 1$, $i = 1,2,\ldots,N$. Here, $P_i(z)$ is the characteristic polynomial of the coefficient matrix in system (11), i.e.,

$$P_i(z) = z^2 + a_i z + b_i, \tag{13}$$

where $a_i = \alpha_i T \sum\limits_{j=1}^{i} w_{ij}D_{ij} - 2$ and $b_i = 1 - \alpha_i T \sum\limits_{j=1}^{i} w_{ij}D_{ij} + \alpha_i T^2 w_{ii} r_i$. Condition i) means that every root of $P_i(z)$ is within a unit circle, which is a necessary and sufficient condition for asymptotic stability of a linear system. Consequently,

$$0 < \alpha_i < \frac{4}{TW_i},$$

$$\max\left\{0, \frac{2(\alpha_i TW_i - 2)}{\alpha_i T^2 w_{ii}}\right\} < r_i < \frac{W_i}{Tw_{ii}}, \tag{14}$$

where $W_i = \sum\limits_{j=1}^{i} w_{ij}D_{ij}$, $i = 1,2,\ldots,N$.

In the above discussion, $G_i(z)$ is the transfer function from $[\mathrm{d}v_{i-1}(n)\ \ \mathrm{d}y_{i-1}(n)\ldots\mathrm{d}y_1(n)]^{\mathrm{T}}$ to $\mathrm{d}v_i(n)$, i.e.,

$$G_i(z) = C(zI_{2\times 2} - A_i)^{-1}B_i = \frac{Q_i(z)}{P_i(z)}, \tag{15}$$

where $Q_i(z) = [T^2\alpha_i w_{ii} r_i \ \ (Ty_0/v_0)\alpha_i w_{i,i-1}D_{i,i-1}r_{i-1}(z-1) \cdots (Ty_0/v_0)\alpha_i w_{i,1}D_{i,1}r_1(z-1)]$. These two conditions guarantee the robust property of the system. That is, the amplitude of the transient disturbance will never be amplified with time. So, the nonjam conditons for the model described by Eqs. (3) and (4) can be summarized as follows:

**Theorem 1** There will be no traffic jams in system (3) and (4) under IVC, if the following conditions are satisfied:

**Condition I**

$$0 < \alpha_i < \frac{-W_i + \sqrt{W_i^2 + 4U_{i-1}\frac{y_0^2}{v_0^2}}}{TU_{i-1}\frac{y_0^2}{v_0^2}},$$

$$\max\left\{0, \frac{\alpha_i TW_i - 1}{\alpha_i T^2 w_{ii}}, R_1\right\} < r_i$$

$$< \min\left\{\frac{W_i}{2Tw_{ii}}, \frac{\alpha_i TW_i - 1}{\alpha_i T^2 w_{ii}}, \frac{\alpha_i(W_i^2 - U_{i-1}\frac{y_0^2}{v_0^2})}{(2 + \alpha_i TW_i)w_{ii}}, R_2\right\};$$

**Condition II**

$$\frac{-W_i + \sqrt{W_i^2 + 4U_{i-1}\frac{y_0^2}{v_0^2}}}{TU_{i-1}\frac{y_0^2}{v_0^2}} \le \alpha_i \le \frac{2}{TW_i},$$

$$\max\left\{0, \frac{\alpha_i TW_i - 1}{\alpha_i T^2 w_{ii}}, \frac{2(\alpha_i TW_i - 2)}{\alpha_i T^2 w_{ii}}\right\} < r_i$$

$$\leq \min\left\{\frac{W_i}{2Tw_{ii}}, \frac{\alpha_i(W_i^2 - U_{i-1}\frac{y_0^2}{v_0^2})}{(2+\alpha_i TW_i)w_{ii}}, R_2\right\};$$

**Condition III**

$$\frac{2}{TW_i} < \alpha_i < \frac{4}{TW_i},$$

$$\max\left\{\frac{W_i}{2Tw_{ii}}, \frac{\alpha_i TW_i - 1}{\alpha_i T^2 w_{ii}}, \frac{2(\alpha_i TW_i - 2)}{\alpha_i T^2 w_{ii}}\right\} < r_i$$

$$< \min\left\{\frac{3W_i}{4Tw_{ii}}, \frac{\alpha_i(W_i^2 - U_{i-1}\frac{y_0^2}{v_0^2})}{(2+\alpha_i TW_i)w_{ii}}, R_2\right\},$$

where

$$W_i = \sum_{j=1}^{i} w_{ij} D_{ij},$$

$$U_{i-1} = \begin{cases} U_0 = 0, & i = 1, \\ \sum_{j=1}^{i-1} w_{ij}^2 D_{ij}^2 r_j^2, & i \geq 2, \end{cases}$$

$$R_1 = \frac{\alpha_i^2 T^2 U_{i-1}\frac{y_0^2}{v_0^2} - \alpha_i^2 T^2 W_i^2 + 4\alpha_i TW_i - 4}{\alpha_i T^2 w_{ii}(2 - \alpha_i TW_i)},$$

$$R_2 = \frac{2 - 2\alpha_i TW_i + \alpha_i^2 T^2 W_i^2 - \alpha_i^2 T^2 U_{i-1}\frac{y_0^2}{v_0^2}}{\alpha_i^2 T^3 W_i w_{ii}}.$$

**Proof** See Appendix A.

## 3. The control method

In order to improve the ability of suppressing traffic jams, a simple feedback control signal $u_i(n)$ is input to model (3):

$$u_i(n) = k(v_{i-1}(n) - v_i(n)), \tag{16}$$

where $k > 0$ is the feedback gain, so

$$v_i(n+1) = \alpha_i\left\{\sum_{j=1}^{i} w_{ij} D_{ij}\left[V_{ij}^{\mathrm{op}}(y_j(n)) - v_i(n)\right]\right\}T + v_i(n) + u_i(n), \tag{17}$$

$$y_i(n+1) = v_{i-1}(n)T - v_i(n)T + y_i(n). \tag{18}$$

Around the steady state, the perturbed system of the controlled model described by Eqs. (17) and (18) can be written by

$$x_i(n+1) = \overline{A}_i x_i(n) + \overline{B}_i q_i(n), \tag{19}$$

$$\mathrm{d}v_i(n) = C x_i(n), \tag{20}$$

where

$$\overline{A}_i = \begin{bmatrix} 1 - T\alpha_i \sum_{j=1}^{i} w_{ij} D_{ij} - k & \frac{Ty_0}{v_0}\alpha_i w_{ii} r_i \\ -\frac{Tv_0}{y_0} & 1 \end{bmatrix} \in R^{2\times 2},$$

$$\overline{B}_i = \begin{bmatrix} k & \frac{Ty_0}{v_0}\alpha_i w_{i,i-1} D_{i,i-1} r_{i-1} & \cdots & \frac{Ty_0}{v_0}\alpha_i w_{i,1} D_{i,1} r_1 \\ \frac{Tv_0}{y_0} & 0 & \cdots & 0 \end{bmatrix} \in R^{2\times N}.$$

The transfer function from $[\mathrm{d}v_{i-1}(n)\ \mathrm{d}y_{i-1}(n)\ \cdots\ \mathrm{d}y_1(n)]^{\mathrm{T}}$ to $\mathrm{d}v_i(n)$ is given by

$$\overline{G}_i(z) = C(zI_{2\times 2} - \overline{A}_i)^{-1}\overline{B}_i = \frac{\overline{Q}_i(z)}{\overline{P}_i(z)}, \tag{21}$$

where

$$\overline{Q}_i(z) = \left[T^2\alpha_i w_{ii} r_i + k(z-1)\ \ \frac{Ty_0}{v_0}\alpha_i w_{i,i-1} D_{i,i-1} r_{i-1}(z-1)\ \ \cdots\ \ \frac{Ty_0}{v_0}\alpha_i w_{i,1} D_{i,1} r_1(z-1)\right],$$

$$\overline{P}_i(z) = z^2 + \overline{a}_i z + \overline{b}_i,\ \ \overline{a}_i = \alpha_i T\sum_{j=1}^{i} w_{ij} D_{ij} - 2 + k,\ \ \overline{b}_i = 1 - \alpha_i T\sum_{j=1}^{i} w_{ij} D_{ij} + \alpha_i T^2 w_{ii} r_i - k.$$

Similarly, in order to suppress traffic jams in the controlled system, the feedback gain $k$ is designed to satisfy the following conditions: a) $P_i(z)$ is stable; b) $\max_{|z|=1} |\, G_i(z) \,| \leq 1$, $i = 1, 2, \ldots, N$.

**Theorem 2** There will be no traffic jams in the controlled system of Eqs. (17) and (18) under IVC, if the following conditions are satisfied:

**Condition I)**

$$0<\alpha_i<\frac{2}{T^2w_{ii}r_i},\ \ \Delta_1\le 0,$$
$$1-\alpha_iTW_i+\alpha_iT^2w_{ii}r_i<k<2-\alpha_iTW_i+\frac{1}{2}\alpha_iT^2w_{ii}r_i;$$

**Condition II)**

$$\begin{aligned}&0<\alpha_i<\frac{2}{T^2w_{ii}r_i},\ \ 0<\Delta_1<(3-2\alpha_iT^2w_{ii}r_i)^2,\\&1-\alpha_iTW_i+\alpha_iT^2w_{ii}r_i<k\\\le\ &\min\{R_{11},2-\alpha_iTW_i+\frac{1}{2}\alpha_iT^2w_{ii}r_i\},\\&k\ne 2-\alpha_iTW_i+\frac{1}{2}\alpha_iT^2w_{ii}r_i;\end{aligned}$$

**Condition III)**

$$\begin{aligned}&0<\alpha_i<\frac{2}{T^2w_{ii}r_i},\ \ \Delta_1\ge(3-2\alpha_iT^2w_{ii}r_i)^2,\\&\max\{R_{12},1-\alpha_iTW_i+\alpha_iT^2w_{ii}r_i\}\\\le\ &k<2-\alpha_iTW_i+\frac{1}{2}\alpha_iT^2w_{ii}r_i,\\&k\ne 1-\alpha_iTW_i+\alpha_iT^2w_{ii}r_i;\end{aligned}$$

**Condition IV)**

$$\begin{aligned}&0<\alpha_i<\frac{4}{T^2w_{ii}r_i},\ \ \Delta_2\le 0,\\&-\alpha_iTW_i+\alpha_iT^2w_{ii}r_i<k\\<\ &\min\{1-\alpha_iTW_i+\alpha_iT^2w_{ii}r_i,2-\alpha_iTW_i+\frac{1}{2}\alpha_iT^2w_{ii}r_i\};\end{aligned}$$

**Condition V)**

$$\begin{aligned}&0<\alpha_i<\frac{4}{T^2w_{ii}r_i},\\&(1-2\alpha_iT^2w_{ii}r_i)^2\le\Delta_2<(3+\alpha_iT^2w_{ii}r_i)^2,\\&\max\{R_{22},-\alpha_iTW_i+\alpha_iT^2w_{ii}r_i\}\\\le\ &k<2-\alpha_iTW_i+\frac{1}{2}\alpha_iT^2w_{ii}r_i,\\&k\ne-\alpha_iTW_i+\alpha_iT^2w_{ii}r_i;\end{aligned}$$

**Condition VI)**

$$\begin{aligned}&0<\alpha_i<\frac{4}{T^2w_{ii}r_i},\ \ 0<\Delta_2<(1-2\alpha_iT^2w_{ii}r_i)^2,\\&-\alpha_iTW_i+\alpha_iT^2w_{ii}r_i<k\le R_{21},\ \text{ or}\\&R_{22}\le k<2-\alpha_iTW_i+\frac{1}{2}\alpha_iT^2w_{ii}r_i,\end{aligned}$$

where

$$\begin{aligned}\Delta_1\ &=\ 9-4\alpha_iTW_i-8\alpha_iT^2w_{ii}r_i\\&\quad+4\alpha_i^2T^3W_iw_{ii}r_i+4\alpha_i^2T^2U_{i-1}\frac{{y_0}^2}{{v_0}^2},\\\Delta_2\ &=\ 1-4\alpha_iTW_i+8\alpha_iT^2w_{ii}r_i\\&\quad+4\alpha_i^2T^3W_iw_{ii}r_i+4\alpha_i^2T^2U_{i-1}\frac{{y_0}^2}{{v_0}^2},\end{aligned}$$

$$\begin{aligned}R_{11}\ &=\ (5-2\alpha_iTW_i-\sqrt{\Delta_1})/2,\\R_{12}\ &=\ (5-2\alpha_iTW_i+\sqrt{\Delta_1})/2,\\R_{21}\ &=\ (1-2\alpha_iTW_i-\sqrt{\Delta_2})/2,\\R_{22}\ &=\ (1-2\alpha_iTW_i+\sqrt{\Delta_2})/2.\end{aligned}$$

A proof is similar to the one given in Appendix A.

The theorem provides the ranges of the feedback gain $k$ under different parameters in the controlled model.

Three differences between our model and the models of Ge[14] and Konishi *et al.*[7] are as follows. Firstly, our model considers the information from a number of preceding vehicles in the realistic inter-vehicle communication (IVC) environment. More precisely, weighted coupled strengths of the transportation network, $w_{ij}$, are used to describe different effects from vehicles in different positions. Secondly, the new model allows vehicles not receiving information from some other vehicles, even if they are in the IVC environment, which is also more realistic. This is done by imposing $D_{ij}=1$ to describe the connected state between two vehicles, which depends on the connectivity $S_{ij}$. Thirdly, in the stability analysis, the perturbed system is studied using the percentage of deviation from the steady state instead of the deviation value, which is more reasonable as compared to other models.

A simulation comparison of our model and the two models of Ge[14] and Konishi *et al.*[7] will be carried out in the next section.

## 4. Simulation and comparison

In this section, computer simulations are performed and compared with two controlled CM car-following models developed previously by Ge[14] and Konishi *et al.*[7]

All the simulations are carried out under open boundary conditions. Uniform parameters are set for the three models as follows:[7]

$$\begin{aligned}&\eta_j=25.0\text{ m},\ \zeta_j=23.3\text{ m},\ v_j^{\max}=33.6\text{ m/s},\\&v^*=20\text{ m/s},\ \alpha_i=2.0\text{ s}^{-1},\\&T=0.1\text{ s},\ y_i^{\min}=7.02\text{ m},\\&i=1,2,\ldots,N;\ j=1,2,\ldots,i.\end{aligned}$$

The analytical model in Ref. [16] is used to calculate the multi-hop connectivity $S_{ij}$ of the IVC system, in which the parameters are set as follows: market penetration rate $\mu=0.1$, transmission range $R=500$ m, $D_{ij}$ randomly obtains the value of 1 by the probability $S_{ij}$, and initial condition is set as the steady state in our model:

$$y_i(0)=y_i^*,\ x_i(0)=\sum_{j=i+1}^{N}y_j^*,\ v_i(0)=v_i^*,\ i=1,2,\ldots,N.$$

Consider a motorcade composed of 100 following vehicles, and let the leading vehicle stop suddenly on four time intervals (in unit s): $nT=100\sim103$, $120\sim123$, $140\sim143$, $160\sim163$ (s). The same external disturbance is given

to Konishi's controlled model, Ge's controlled model, our CM model, and our controlled model, so as to compare their performances. In our controlled model (17), the feedback gain $k$ is obtained by calculation, such that all the parameters fit the condition VI) in Theorem 2, giving $0.7951 \leq k < 0.8944$. The feedback gains in Konishi's and Ge's controlled models can be found from Refs. [7] and [14], respectively, for comparison.

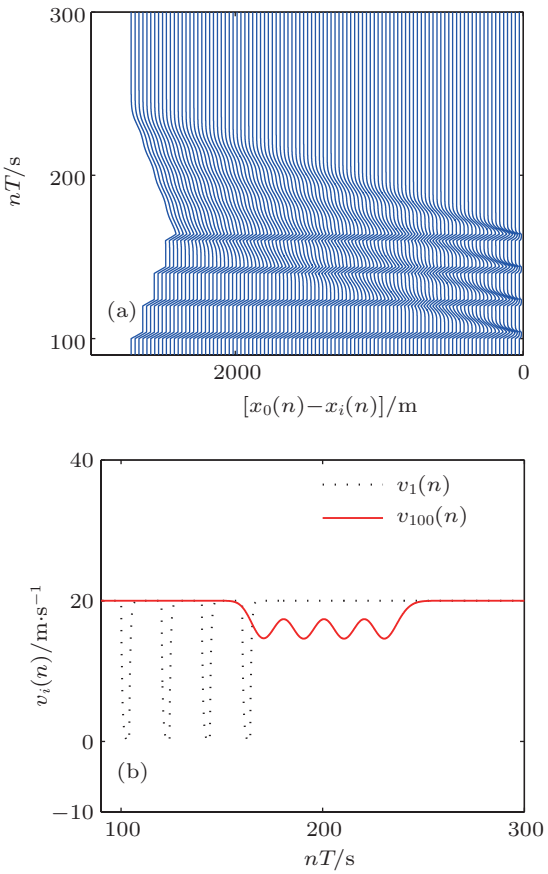



**Fig. 3.** (color online) Simulation results on Konishi's controlled model when the leading vehicle stops suddenly at $nT = 100$ s $\sim$ 103 s, 120 s $\sim$ 123 s, 140 s $\sim$ 143 s, 160 s $\sim$ 163 s. (a) The space–time plot, (b) the variations of velocities of the 1st and 100th vehicles.

The results of simulations on Konishi's controlled (KKHC) model, Ge's controlled (GC) model, our CM (IVC-CM) model, and our controlled (IVC-CMC) model are shown in Figs. 3, 4, 5, and 6, respectively. All the sub-figures labeled (a) show the space–time plots of the running traffic after $nT = 90$ s. The horizontal axises represent the distances between the leading vehicle and all the following vehicles. All the sub-figures labeled (b) illustrate the variations of velocities of the 1st and 100th vehicles. It can be seen that the disturbance due to sudden stops propagates backward. From Figs. 3(a)–6(a), it can be seen that our uncontrolled and controlled models and Ge's controlled model have better performances in suppressing traffic jams than Konishi's controlled model. From Figs. 3(b)–6(b), one can also see that the velocity of the 100th vehicle in our model oscillates much smaller than the ones in Konishi's and Ge's controlled models. Especially, from Figs. 4(b) and 5(b), it can be observed that the 100th vehicle in our model starts to decelerate much earlier, meanwhile the maximum deviation of the velocity from the steady state is also smaller than that in Ge's controlled model. Specifically, some parameters' values obtained from simulations are given in Table 1 to compare the velocity fluctuations of the 100th vehicle for the four models. In Table 1, $\bar{a}_{\text{half}_{100}}$ is the average acceleration from $t_1 = 90$ s to $t_2$, i.e.,

$$\bar{a}_{\text{half}_{100}} = \frac{\sum_{nT=t_1}^{t_2} |a_{100}(nT)|}{t_2 - t_1 + 1},\ nT = t_1, t_1+1, \ldots, t_2,$$

where $t_2$ is the moment when the vehicle's velocity reaches the maximal deviation from the steady state, and $|a_{100}(nT)|$ is the absolute value of acceleration at time $t = nT$; $\bar{a}_{\text{whole}_{100}}$ is the average acceleration from $t_1 = 90$ s to $t_3 = 300$ s, i.e.,

$$\bar{a}_{\text{whole}_{100}} = \frac{\sum_{nT=t_1}^{t_3} |a_{100}(nT)|}{t_3 - t_1 + 1},\ nT = t_1, t_1+1, \ldots, t_3;$$

in which $\Delta v_{\max}$ is the maximum deviation of the velocity from the steady state; $T_{p_{100}}$ is the time interval during which the 100th vehicle's velocity deviates from the region of stability and comes back to it. The region is defined as $[v^*_{100} - 0.5, v^*_{100} + 0.5]$.

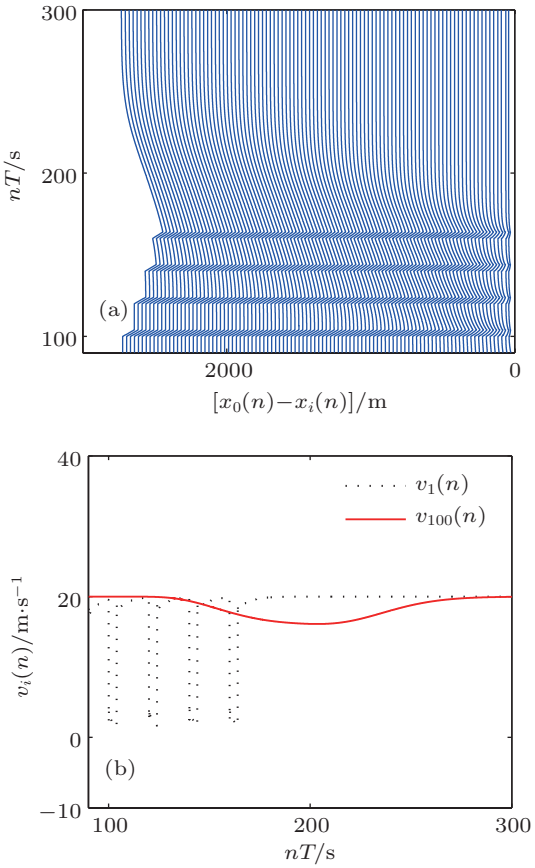



**Fig. 4.** (color online) Simulation results on Ge's controlled model when the leading vehicle stops suddenly at $nT = 100$ s $\sim$ 103 s, 120 s $\sim$ 123 s, 140 s $\sim$ 143 s, 160 s $\sim$ 163 s. (a) The space–time plot, (b) the variations of velocities of the 1st and 100th vehicles.

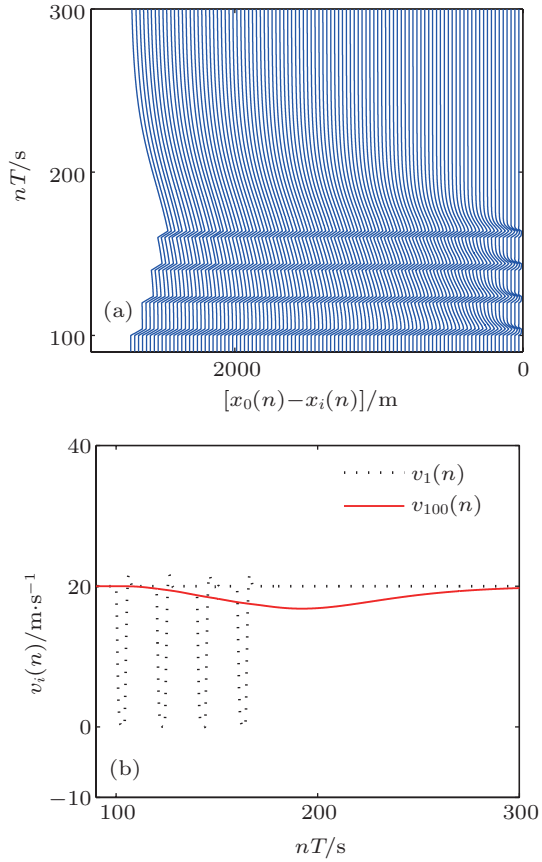



**Fig. 5.** (color online) Simulation results on the new CM car-following model when the leading vehicle stops suddenly at $nT = 100$ s $\sim$ 103 s, 120 s $\sim$ 123 s, 140 s $\sim$ 143 s, 160 s $\sim$ 163 s. (a) The space–time plot, (b) the variations of velocities of the 1st and 100th vehicles.

It can be clearly seen that the 100th vehicle runs more smoothly in our models. Of course, it should be noted that the first vehicle in our uncontrolled model oscillates larger than that in Ge's model. However, from Fig. 6(b) it can be seen that our controlled model has no such a problem. In summary, these simulations show that all the four models can be used to suppress traffic jams, yet nevertheless our controlled model has better performances than other three models overall.

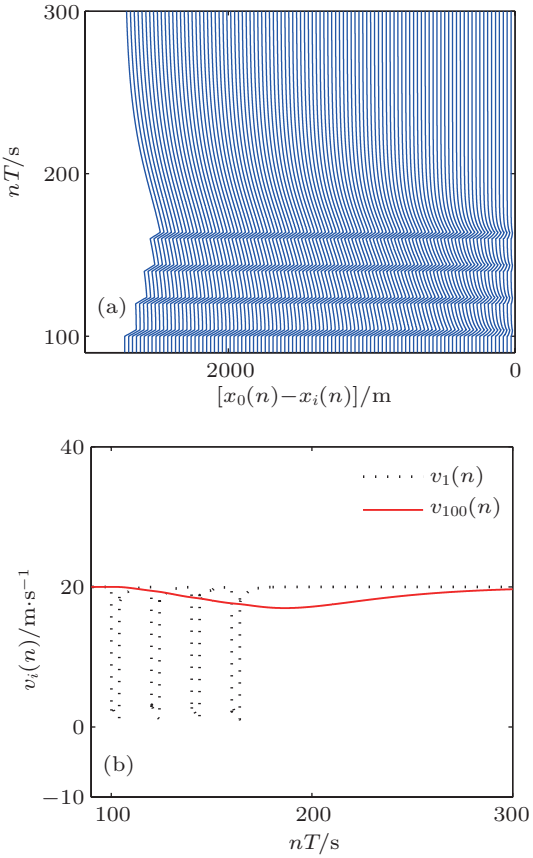



**Fig. 6.** (color online) Simulation results on the controlled model in this paper when the leading vehicle stops suddenly at $nT = 100$ s $\sim$ 103 s, 120 s $\sim$ 123 s, 140 s $\sim$ 143 s, 160 s $\sim$ 163 s. (a) The space–time plot, (b) the variations of velocities of the 1st and 100th vehicles.

**Table 1.** Comparison of four models about the velocity fluctuation of the 100th vehicle.

| Model | $\bar{a}_{\text{half}_{100}}$/(m/s$^2$) | $\bar{a}_{\text{whole}_{100}}$/(m/s$^2$) | $\Delta v_{\max_{100}}$/(m/s) | $T_{p_{100}}$/s |
|---|---|---|---|---|
| KKHC | 0.1357 | 0.1305 | 5.3928 | 86.1 |
| GC | 0.0341 | 0.0372 | 3.8893 | 127.1 |
| IVC-CM | 0.0315 | 0.0292 | 3.1784 | 156.6 |
| IVC-CMC | 0.0313 | 0.0272 | 3.0076 | 166.6 |

## 5. Conclusion

In this paper, a new coupled map car-following model with inter-vehicle communication (IVC) is proposed, and a simple control method for the new model is suggested. The stability of the uncontrolled and controlled models is investigated, with nonjam criteria derived. Through theoretical analysis and computer simulations, we conclude that: a) our models are proposed under the framework of supernetwork, representing the interaction between the transportation network and communication network, which are more realistic than some existing models. b) The stability of the traffic system is improved by considering the effect of numerous preceding vehicles' information in the new model. c) Numerical simulations demonstrate that the traffic flow of our uncontrolled and controlled models run smoothly, and have good performances on suppressing the traffic jams, which is consistent with the theoretical analysis. Compared with two classical controlled CM models studied in Refs. [7] and [14] with the same set of parameters, our controlled model performs better overall.

In this paper, it is assumed that the connectivity of the communication network is constant while the transportation network is dynamic. In future studies, it is desirable to inves-

tigate two dynamic networks under the supernetwork framework, taking into account of their interactions and dynamic evolutions. Besides, the framework of a supernetwork based on communication network and transportation network is an important topic for future investigation. It could be applied to the two-dimensional models of traffic flows, which will contribute to alleviating actual traffic congestion.

## Appendix A

Firstly, according to the classical stability criterion, $P_i(z)$ is stable if $|b_i|<1$, $|a_i|<1+b_i$. One can obtain

$$0<\alpha_i<\frac{4}{TW_i},\quad \max\left\{0,\frac{2(\alpha_iTW_i-2)}{\alpha_iT^2w_{ii}}\right\}<r_i<\frac{W_i}{Tw_{ii}}. \tag{A1}$$

Then, consider $\max\limits_{|z|=1}\mid G_i(z)\mid\leq 1$, where

$$\mid G_i(z)\mid=\sqrt{G_i(z)G_i^{\mathrm{T}}(\overline{z})},\quad i=1,2,\ldots,N.$$

One has

$$\begin{aligned}&2(1-\cos\theta)\Big[(-2+2\alpha_iTW_i-2\alpha_iT^2w_{ii}r_i)\cos\theta\\&\quad+2-2\alpha_iTW_i+\alpha_i^2T^2W_i^2\\&\quad-\alpha_i^2T^3W_iw_{ii}r_i-T^2\alpha_i^2U_{i-1}\frac{y_0^2}{v_0^2}\Big]\geq 0.\end{aligned} \tag{A2}$$

Since $\forall\theta\in[0,2\pi]$, $1-\cos\theta\geq 0$, the above inequality is equivalent to

$$\begin{aligned}&(-2+2\alpha_iTW_i-2\alpha_iT^2w_{ii}r_i)\cos\theta+2-2\alpha_iTW_i\\&\quad+\alpha_i^2T^2W_i^2-\alpha_i^2T^3W_iw_{ii}r_i-T^2\alpha_i^2U_{i-1}\frac{y_0^2}{v_0^2}\geq 0.\end{aligned}$$

Let

$$\begin{aligned}g_i(\theta)=&(-2+2\alpha_iTW_i-2\alpha_iT^2w_{ii}r_i)\cos\theta\\&+2-2\alpha_iTW_i+\alpha_i^2T^2W_i^2\\&-\alpha_i^2T^3W_iw_{ii}r_i-T^2\alpha_i^2U_{i-1}\frac{y_0^2}{v_0^2}.\end{aligned}$$

It is clear that if the following conditions are satisfied:

C1) when $-2+2\alpha_iTW_i-2T^2\alpha_iw_{ii}r_i>0$, $g_i(\theta)_{\min}=g_i(\pi)\geq 0$;

C2) when $-2+2\alpha_iTW_i-2T^2\alpha_iw_{ii}r_i<0$, $g_i(\theta)_{\min}=g_i(0)\geq 0$;

C3) when $-2+2\alpha_iTW_i-2T^2\alpha_iw_{ii}r_i=0$, $g_i(\theta)\geq 0$,

then the inequality (A2) holds.

Finally, synthesizing the results derived from the above three conditions, C1–C3, and the inequality (A1), the theorem is proved.

## References


[1] Pipes L A 1953 *J. Appl. Phys.* **24** 274
[2] Pipes L A 1967 *Trans. Res.* **1** 21
[3] Newell G F 1961 *Oper. Res.* **9** 209
[4] Bando M, Hasebe K, Nakayama A, Shibata A and Sugiyama Y 1995 *Phys. Rev. E* **51** 1035
[5] Helbing D and Tilch B 1998 *Phys. Rev. E* **58** 133
[6] Jiang R, Wu Q S and Zhu Z J 2010 *Transp. Res. B* **36** 405
[7] Konishi K, Kokame H and Hirata K 1999 *Phys. Rev. E* **60** 4000
[8] Zhao X M and Gao Z Y 2006 *Physica A* **366** 513
[9] Han X L, Jiang C Y, Ge H X and Dai S Q 2007 *Acta Phys. Sin.* **56** 4383 (in Chinese)
[10] Han X L, Li X L and Jiang C Y 2009 *J. Transpn. Sys. Eng. & I.T.* **9** 62
[11] Ge H X, Cheng R J and Li Z P 2011 *Acta Phys. Sin.* **60** 080508 (in Chinese)
[12] Shen F Y, Zhang H, Ge H X, Yu H M and Lei L 2009 *Chin. Phys. B* **18** 4208
[13] Yu H M, Cheng R J and Ge H X 2010 *Commun. Theor. Phys.* **54** 117
[14] Ge H X 2011 *Chin. Phys. B* **20** 090502
[15] Ge H X, Dai S Q, Dong L Y and Xue Y 2004 *Phys. Rev. E* **70** 066134
[16] Ge H X, Dai S Q, Dong L Y and Dong L Y 2006 *Physica A* **365** 543
[17] Peng G H and Sun D H 2009 *Chin. Phys. B* **18** 5420
[18] Peng G H 2010 *Chin. Phys. B* **19** 056401
[19] Sun D H, Liao X Y and Peng G H 2011 *Physica A* **390** 631
[20] Jin W L and Recker W W 2010 *IEEE Trans. Wireless Comm.* **1** 106
[21] Nagurney A and Dong J 2002 *Supernetworks: Decision-Making for the Information Age* (Cheltenham: Edward Elgar Press)